Flow Instabilities in Entangled Polymer Thin Films

Jean-Loup Masson, Okikiolu Olufokunbi, and Peter F. Green*

Texas Materials Institute and Chemical Engineering Department, The University of Texas at Austin, Austin, Texas 78712

Received January 31, 2002

ABSTRACT: The line of contact at the moving front of a simple liquid on a substrate can become unstable toward the formation of fingers under the action of an external force, such as a temperature gradient or a mechanical force. During the dewetting of entangled polymeric liquid thin films, the moving front (rim) of a growing hole can become unstable toward the formation of fingers in the absence of an external driving force. In this paper we show that instabilities develop at the line of contact, leading to the formation of fingers, in films below a critical film thickness, h_c. The extent of fingering decreases as the film thickness increases and virtually disappears for $h > h_c$. This critical film thickness increases with increasing molecular weight, approximately as $h \sim M^{3/7}$. Our observations are rationalized in terms of a rough scaling argument.

Introduction

Thin organic or polymeric films are important for numerous technological applications, including coatings, lubrication, and various organic electronic devices and sensors. Ultrathin films (h < 100 nm) on nonwettable substrates can become unstable and rupture, creating a series of patterns reflecting fluctuations in local film thickness.[1−8] Rupturing exposes the underlying substrate and often leads to the nucleation of circular holes that subsequently grow under the action of capillary forces. The chains removed during growth accumulate at the periphery of the hole to form a rim. The growth of circular holes, with stable rims, on substrates is reasonably well understood theoretically[9,10] and experimentally.[11,12] Typically, the flow of an entangled polymer melt on a substrate can be accommodated by "slip" along the polymer/substrate interface with a finite velocity, V.[13] Slippage is characterized by a hydrodynamic extrapolation, or slippage length, b, defined by the ratio of the viscosity, η, of the polymer to the friction coefficient, k, at the interface (the shear stress at the interface is $\sigma = kV$). Under these conditions, unlike simple liquids, the dissipation associated with flow is assumed to occur primarily at the substrate/liquid interface. Consequently, flow is restricted to the vicinity of the moving liquid front, and a rim (or a ridge) forms at the front due to accumulation of polymer chains. When dissipation occurs primarily at the substrate/polymer interface, the velocity of the contact line is constant[9] and

$$V_g = \frac{|S|}{\eta}\left(\frac{b}{h}\right)^{1/2} \quad (1)$$

In this expression, h is the initial film thickness and S is the spreading coefficient of the liquid on the substrate. Equation 1 is valid if the displacement of the contact line is smaller than the slippage length, b (b can on the order of many micrometers for long-chain polymers). This indicates the dependence of the velocity of growth on the slippage length and therefore the molecular weight. Other growth laws of dewetting have been proposed to address situations of partial slippage.[10]

In this paper we are particularly interested in the situation in which the rim does not remain stable during the growth process. Fluctuations may develop in the shape of the rim as the holes grow and fingers develop inside the hole, as illustrated in Figure 1. Similar phenomena have been observed in other systems in the absence of external forces and have been compared to a Plateau−Rayleigh instability.[4,14−16] Fingering instabilities are well documented in simple liquid films where they occur only under forced spreading conditions. Forced spreading conditions include spreading subject to Marangoni flows (temperature gradients in surface tension) or to gravitational forces acting on a liquid moving down an incline.[17−19]

In this paper we investigate rim instabilities that occur during the dewetting of *entangled* polystyrene thin films from SiO_x/Si substrates. During the dewetting process, holes nucleate throughout the film and grow under capillary forces. We show that if the film is below a certain threshold film thickness, h_c, the rim becomes unstable after a certain period of growth, and fingers develop. Above a certain film thickness, the fingering is not observed, and the holes grow and eventually impinge, forming ribbons, which subsequently decay to droplets due to a Rayleigh instability. The threshold thickness is molecular weight dependent. We rationalize our observations in terms of a simple scaling argument.

Experimental Section

We examined the dewetting of thin polystyrene (PS) films of molecular weight, M, ranging from 49 to 1600 kg/mol from silicon substrates. PS films were prepared on silicon substrates (with native SiO_x layers of 2 nm) by spin-coating toluene solutions. The films were subsequently annealed at 170 °C in a vacuum for various times unless indicated otherwise. Images of holes in the films, quenched to room temperature, were made periodically using an Autoprobe CP atomic force microscope (AFM), manufactured by Thermomicroscopes, in contact mode. Note that AFM scans of the same regions of the sample were made each time in order to make an accurate assessment of how the morphology of individual holes developed as a function of time. Further details of our experiments can be found in separate publications.[6,7,10,11]

Results

Molecular Weight Dependence of a Rim Instability. We performed numerous measurements of films

10.1021/ma020161i CCC: $22.00
Published on Web 07/26/2002

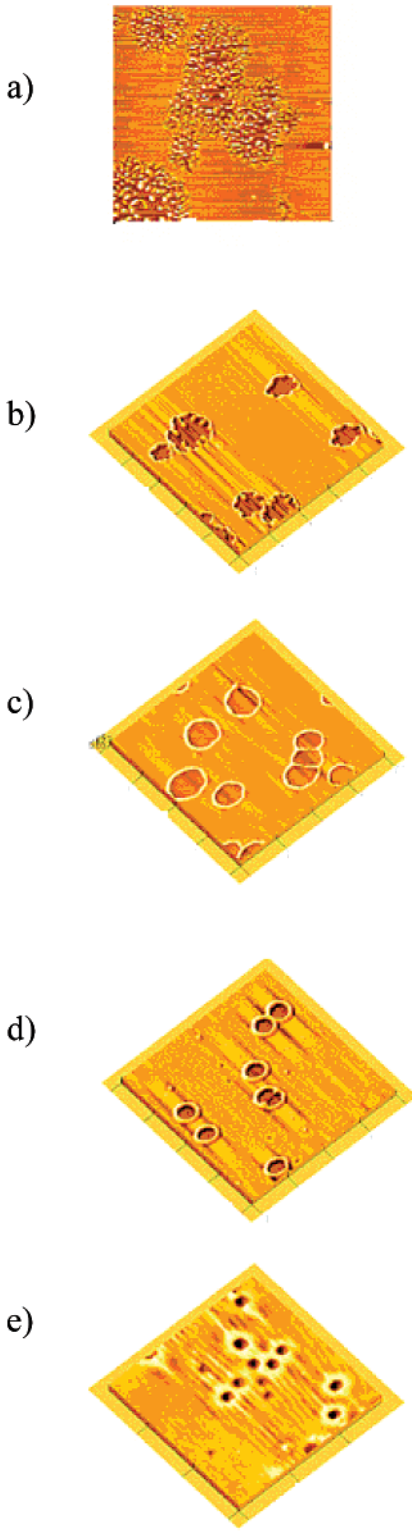

Figure 1. This series of AFM images shows that fingering develops at the edges of moving fronts of holes growing in thin film PS films a nonwettable substrate. The instability is suppressed with increasing film thickness. The molecular weight of the polystyrene is $M = 130$ kg/mol films, and the temperature is 170 °C. (a) $h = 10$ nm (60 μm × 60 μm); (b) $h = 17$ nm (80 μm × 80 μm); (c) $h = 29$ nm (80 μm × 80 μm) (d) $h = 40$ nm (80 μm × 80 μm); (e) $h = 102$ nm (80 μm × 80 μm) (holes do not reach the substrate). With increasing h, the samples had to be annealed for increasingly longer times to achieve comparable hole diameters.

of varying thicknesses using polystyrenes of varying molecular weights in the entanglement regime. The

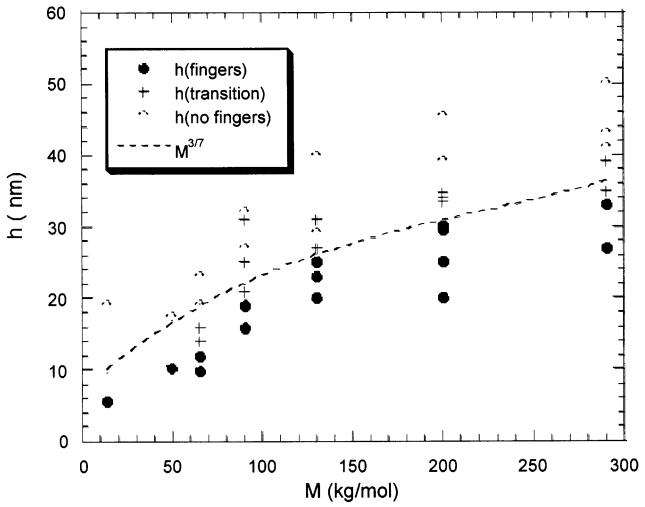

Figure 2. A map of the fingering instability as a function of the initial film thickness, h, for samples of varying molecular weight, M. The line separating the regions of film thickness where fingers are present or absent corresponds to the theoretical prediction $h_c \propto M^{3/7}$.

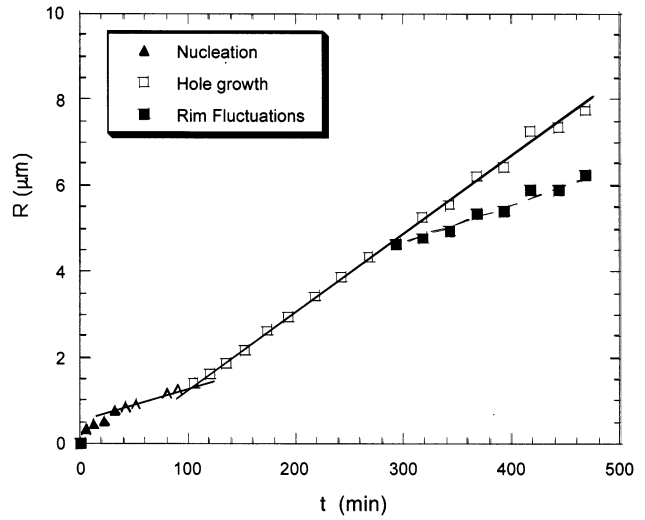

Figure 3. Nucleation and growth stages for a hole in a thin film of $h = 32$ nm for PS of $M = 130$ kg/mol at 180 °C. The growth stage occurs for $t > 100$ min, and fluctuations in the shape of the rim become important for $t > 300$ min.

images in Figure 1 show how the morphology of holes in thin polystyrene ($M = 130$ kg/mol) films change with increasing film thickness for films which increased in thickness from $h = 10$ to 102 nm. Instabilities (fingering) develop in the rims at the perimeters of growing holes. The images in this figure clearly indicate that as the film thickness increases, the film becomes more stable toward the formation of fingers for hole diameters of comparable sizes. These images strongly suggest that there exists a thickness threshold beyond which the fingering instability does not develop.

For each molecular weight there exists a characteristic film thickness, h_c, beyond which the fingering instabilities were suppressed. The threshold film thickness increased with increasing molecular weight, as shown in Figure 2. The open symbols in this figure identify film thicknesses in which fingering instabilities did not develop. The filled circles, on the other hand, were obtained from films in which fingering instabilities were observed. There exists a transition regime, denoted by the + symbols, in which the rim fluctuated in shape,

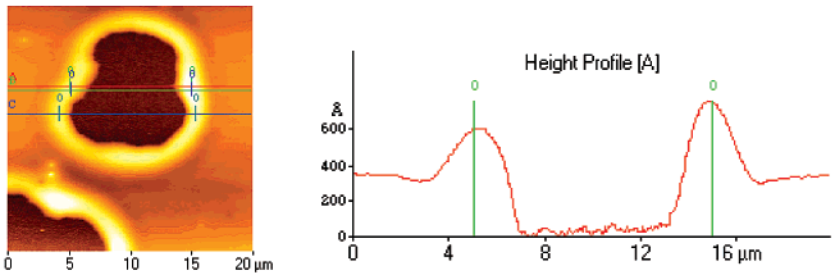

Figure 4. An image showing the fluctuation in the shape of the rim during the early stage, at $t = 345$ min, for the hole whose dynamics are described in Figure 3.

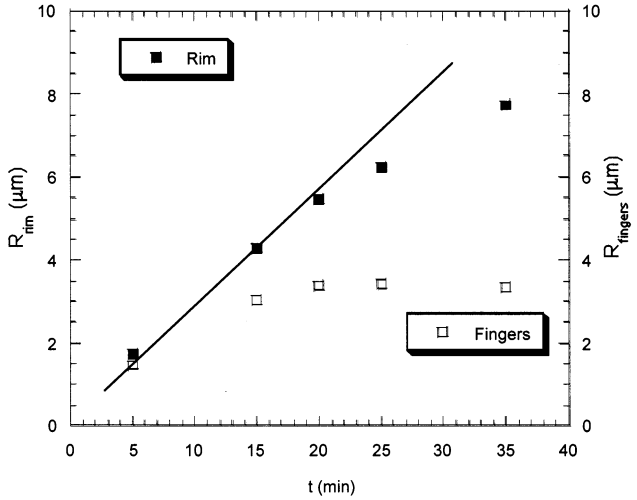

Figure 5. Position of the moving fronts (rim and fingers) as a function of time in a film of thickness $h = 17$ nm, molecular weight 130 kg/mol, and annealed at $T = 170$ °C.

but fingering did not occur. This transition regime appears to be well-defined, as shown in the figure, and is clearly molecular weight dependent. We also observed that the holes grew at a faster rate in thinner films.[11] When the films were sufficiently thick, the holes do not reach the substrate.[12] Later we will discuss the possible origin of this molecular weight dependence of h_c. However, we first address the time-dependent evolution of the hole morphology of the samples.

Time-Dependent Evolution of a Hole That Exhibits a Rim Instability. We begin describing the hole formation and growth process in the *transition* regime. Initially, a local fluctuation develops in the film, creating a depression. The depth of this depression increased with time, as illustrated in Figure 3 for a film of $h = 32$ nm at $T = 180$ °C. At time $t = 100$ min, the depression reached the substrate. The radius of the hole during this nucleation stage is characterized by two different time dependencies. We will not discuss this regime further here since it is the subject of an earlier publication.[12]

The important message from the data in this figure is that the fluctuations in the shape of the rim occur during the linear growth regime, for $t > 300$ min. Two sets of data, open and filled squares, are shown for $t > 300$ min. The open squares in the figure were determined by measuring the average distance from the center of the hole to the rim. The amplitude of the fluctuations of the shape of the rim is not uniform throughout the entire perimeter of the hole. In fact, the region of the perimeter of the hole where the fluctuations first appear have the largest amplitude. The filled squares represent the average distance between the center of the hole and the distance of closest approach of the line of contact of the rim.

For film thicknesses below the transition regime, fluctuations in the shape of the rim lead to the formation of fingers. The data in Figure 5 illustrate the time dependence of the process in films of $h < h_c$. Here fingering develops for $R > 2$ μm. The filled squares indicate the average radius of a hole, and the open squares represent the distance between the center of the hole and the point of contact of the closest finger. The fingers increase in length as the average radius of the hole increases. As the average radius increased, the velocity of the line of contact of the fingers eventually becomes zero due to the rupturing of thin threads of the viscoelastic liquid into droplets.

Discussion

Holes appear throughout the film as a result of rupturing, and they subsequently grow on a nonwetting substrate. The driving force for growth of the holes is the spreading coefficient, $S = \gamma_{sv} - (\gamma_{ps} + \gamma_{pv})$, which is negative. In this expression, γ_{sv}, γ_{ps}, and γ_{pv} are the surface tension of the substrate, the interfacial tension of polymer/substrate interface, and polymer/vacuum interfacial tension, respectively. As the hole grows, a circular rim develops at the perimeter of the hole due to the accumulation of chains. The existence of the rim is a result of the fact that frictional forces at the substrate/liquid interface oppose the movement of the liquid film on the substrate. Whereas the driving force for spreading is constant during hole growth, the friction forces increases with the size of the rim. However, the developing rim instability removes polymer from the rim, therefore reducing the rim width and, hence, the frictional forces. Reiter highlighted the auto-optimization of dewetting rates (constant dewetting velocity) by rim instabilities in slipping polymer films.[14] The decrease in the velocity of the rim in Figure 5 is therefore attributed to the increasing asymmetry of the rim that creates hindrances to the hole growth.

During hole growth, the rim grows in height and width in a cylindrical-like shape and is unstable toward instabilities reminiscent of Rayleigh instabilities.[16] The amplitude of the fluctuations increase until fingers form within the interior of the growing hole. In our experiments, we observed an apparent thickness threshold above which the rim instability was suppressed. Note that fluctuations develop in the shape of the rim and larger regions of the rim move at a slower rate than thinner ones as the hole increases in size. For the thinnest films, $h < h_c$, the rim is small and the hole velocity is large, comparatively. Under these conditions the fluctuations are amplified and fingers develop. With increasing film thickness (accompanied by an increasing

rim size) coupled with the decreasing growth velocity, the size of the fluctuations decrease and the fingering is suppressed. We also note that an isolated hole would develop fingers only if the radius of the hole is sufficiently large. Earlier, Brochard et al. earlier developed theory for rim instabilities in thin films.[16] This theory, however, is not valid for our case because our system is entangled and slip plays an important role. Below we make attempt at a simple analysis that enables a prediction that is relevant to our experimental system.

It is generally understood that fingering instabilities occur at the line of contact of viscous liquids that spread due to an external driving force, such as spreading of a liquid on an inclined plane under the influence of gravitational forces[17] or spreading due to centrifugal forces[18] or to Marangoni forces (gradients in surface tension).[19] The forces due to the spreading coefficient are always negligible compared to the applied forces and do not play a role in such systems. Fingering instabilities occur when fluctuations at the liquid front are amplified by surface tension, γ. Specifically, variations of the film thickness profile (rim height) near the line of contact results in a Laplace pressure that produces a surface curvature flow that contributes to pressure gradients.

We can perform a simple scaling analysis to determine the relationship between film thickness, molecular weight, and a characteristic length scale associated with fingering. The velocity gradients can be written in terms of the pressure gradients for steady-state flow in the radial direction for a thin film, within the lubrication approximation, as[20]

$$\eta \frac{\partial^2 V_r}{\partial z^2} \sim \frac{\partial p}{\partial r} \tag{2}$$

V_r is a velocity in the radial direction, p is the pressure in the film near the line of contact, and η is the viscosity. This equation is generally applicable to slip and nonslip conditions. For small surface curvature we can write $\partial p/\partial x = -\gamma(\mathrm{d}^3h/\mathrm{d}r^3)$, where γ is the surface tension, so

$$\eta \frac{\partial^2 V_r}{\partial z^2} \approx -\gamma \frac{\mathrm{d}^3 h}{\mathrm{d}r^3} \tag{3}$$

It follows that the right-hand side of this equation describes flow due to surface curvature (Laplace pressure). It is typical to define a length scale, L, over which the capillary forces influence flow in the film from the moving front.[19] With this in mind one can proceed as follows:[21]

$$\eta \frac{V_r}{{h_0}^2} \sim \gamma \frac{h_0}{L^3} \tag{4}$$

If this length scale, L, is proportional to the wavelength, λ,[22] associated with fingering, then

$$\lambda \sim (Ca)^{-1/3} h_0 \tag{5}$$

The term in parentheses is a capillary number $Ca = \eta V_r/\gamma$. This equation is not new and was found to characterize length scales associated with fingering instabilities for flow driven by Marangoni forces (temperature gradients in surface tension)[18,22] or by gravitational forces down an incline.[17]

If we now substitute eq 1 for the velocity of the film at the line of contact, then we arrive at an expression relating λ, molecular weight, and film thickness:

$$\lambda \sim \left(\frac{M_e \gamma}{|S|}\right)^{1/3} \frac{h^{7/6}}{M^{1/2}} \tag{6}$$

In arriving at eq 6, we used the fact that the extrapolation length b is proportional to M^3/M_e^2. Equation 6 predicts that the wavelength of the instability decreases as $M^{-1/2}$. In typical fingering experiments, one would measure the wavelength of the instabilities. However, in our experiments we encountered a very new phenomenon; fingering appeared only when the film was below a critical film thickness, and this critical film thickness was a function of molecular weight (Figure 2). In other words, entangled polymeric liquids moving along a nonwetting substrate are more susceptible to fingering instabilities than are simple, nonpolymeric liquids. While viscoelastic effects should stabilize the shape of the rim at the line of contact, slippage appears to have a more dominant destabilizing effect.[23]

All our data indicate that as the film became thicker, the shape of the rim became more stable. Note that if we assume that there exists a constant wavelength, λ_c, beyond which the system become stabilized and the fingering is suppressed, then we can predict a molecular weight dependence of h_c. This wavelength would be associated with the distance between fingers (see Figure 1b). With this in mind, eq 6 would predict that $h_c \sim M^{3/7}$. The agreement is interesting, and clearly it is necessary to perform other experiments to determine the wavelength as a function of M. We note that the $M^{3/7}$ dependence comes from the fact that we assumed that $b \sim \eta \sim M^3$. Using the empirical result that $\eta \sim M^{3.4}$ would have yielded a $M^{1/2}$ dependence, which would also have described our data. A more detailed series of calculations must be done by theorists in the future.

Concluding Remarks

We showed that in sufficiently thin polymer films the line of contact between the polymer and a nonwettable substrate can unstable toward the formation of fingers under normal flow conditions, where the driving force is due entirely to capillarity, opposed by the viscous forces. Specifically, during the growth stage of hole that nucleates in a thin film chains accumulate at the perimeter of the hole to form a rim. The average size, thickness, of the rim increases with film thickness for the holes that nucleate. Fluctuations develop in the shape of the rim, and larger regions of the rim move at a slower rate than thinner ones as the hole increases in size. For the thinnest films, $h < h_c$, the rim is small and the hole velocity is large, comparatively. Under these conditions the fluctuations are amplified and fingers develop. With increasing film thickness, and rim size, coupled with the decreasing growth velocity, the sizes of the fluctuations decrease, and the fingering is suppressed when $h \sim h_c$. While fluctuations in the shape of the rim are observed in the transition regime, fingers do not develop. The holes impinge before this occurs. When the film becomes thicker, the rims are larger and are therefore not subject to the destabilizing fluctuations.

We were able to rationalize the molecular weight dependence on the basis of the fact that the velocity of hole growth depends on the extrapolation length, b, and

that the instability, like typical fingering instabilities, is characterized by a length scale λ which is determined by a film thickness and a capillary number. These considerations lead to the predicted molecular weight dependencies.

Acknowledgment. This work was supported by the National Science Foundation (DMR-9705101) and the Robert A. Welch Foundation. P.F.G. acknowledges Venkat Ganesan and Roger Bonnecaze for helpful discussions.

References and Notes

(1) Brochard-Wyart, F.; Daillant, J. *Can. J. Phys.* **1990**, *68*, 1084.
(2) Kheshgi, H. S.; Scriven, L. E. *Chem. Eng. Sci.* **1991**, *46*, 519.
(3) Reiter, G. *Phys. Rev. Lett.* **1992**, *68*, 75.
(4) Reiter, G. *Langmuir* **1993**, *9*, 1344.
(5) Xie, R.; Karim, A.; Douglas, J. F.; Han, C. C.; Weiss, R. A. *Phys. Rev. Lett.* **1998**, *81*, 125.
(6) Masson, J.-L.; Green, P. F. *J. Chem. Phys.* **2000**, *112*, 349.
(7) Limary, R.; Green, P. F. *Langmuir* **2000**, *15*, 5617.
(8) Segalman, R.; Green, P. F. *Macromolecules* **1999**, *32*, 808.
(9) Brochard-Wyart, F.; Debrégeas, G.; Fondecave, R.; Martin, P. *Macromolecules* **1997**, *30*, 1211.
(10) Jacobs, K.; Herminghaus, S.; Mecke, K. R. *Langmuir* **1998**, *14*, 965.
(11) Masson, J.-L.; Green, P. F. *Phys. Rev. E* **2002**, *65*, 031806.
(12) Masson, J.-L.; Green, P. F. *Phys. Rev. Lett.* **2002**, *88*, 205504.
(13) De Gennes, P. G. *Rev. Mod. Phys.* **1985**, *57*, 827.
(14) Reiter, G.; Sharma, A. *Phys. Rev. Lett.* **2001**, *87*, 166103-1.
(15) Herminghaus, S.; Fery, A.; Schlagowski, S.; Jacobs, K.; Seemann, R.; Gau, H.; Mönch, W.; Pompe, T. *J. Phys.: Condens. Matter* **1999**, *11*, A57.
(16) Brochard-Wyart, F.; Redon, C. *Langmuir* **1992**, *8*, 2324.
(17) Huppert, H. E. *Nature (London)* **1982**, *300*, 427.
(18) Melo, F.; Joanny, J. F.; Fauve, S. *Phys. Rev. Lett.* **1989**, *63*, 1958.
(19) Cazabat, A. M.; Heslot, F.; Troian, S. M.; Carles, P. *Nature (London)* **1990**, *346*, 824.
(20) Bird, R. B.; Stewart, W. E.; Lightfoot, E. N. *Transport Phenomena*; Wiley: New York, 1976.
(21) Tritton, D. J. *Physical Fluid Dynamics*; Van Nostrant Reinhold: New York, 1977.
(22) Troian, S. M.; Herbolzheimer, E.; Safran, S. A.; Joanny, J. F. *Europhys. Lett.* **1989**, *10*, 25.
(23) Spaid, M. A.; Homsy, G. M. *Phys. Fluids* **1996**, *8*, 460.

MA020161I